Phytoplankton trigger the production of cryptic metabolites in the marine actinobacteria *Salinispora tropica*.

Audam Chhun[1,#], Despoina Sousoni[1], Maria del Mar Aguiló-Ferretjans[2], Lijiang Song[3], Christophe Corre[1,3,#], Joseph A. Christie-Oleza[1,2,4,#]

[1] School of Life Sciences, University of Warwick, Coventry, UK
[2] University of the Balearic Islands, Palma, Spain
[3] Department of Chemistry, University of Warwick, Coventry, UK
[4] IMEDEA (CSIC-UIB), Esporles, Spain

[#]Corresponding authors: a.chhun@warwick.ac.uk, c.corre@warwick.ac.uk and joseph.christie@uib.eu

---

Abstract

Bacteria from the Actinomycete family are a remarkable source of natural products with pharmaceutical potential. The discovery of novel molecules from these organisms is, however, hindered because most of the biosynthetic gene clusters (BGCs) encoding these secondary metabolites are cryptic or silent and are referred to as orphan BGCs. While co-culture has proven to be a promising approach to unlock the biosynthetic potential of many microorganisms by activating the expression of these orphan BGCs, it still remains an underexplored technique. The marine actinobacteria *Salinispora tropica*, for instance, produces valuable compounds such as the anti-cancer molecule salinosporamide A but half of its putative BGCs are still orphan. Although previous studies have looked into using marine heterotrophs to induce orphan BGCs in *Salinispora*, the potential impact of co-culturing marine phototrophs with *Salinispora* has yet to be investigated. Following the observation of clear antimicrobial phenotype of the actinobacterium on a range of phytoplanktonic organisms, we here report the discovery of novel cryptic secondary metabolites produced by *S. tropica* in response to its co-culture with photosynthetic primary producers. An approach combining metabolomics and proteomics revealed that the photosynthate released by phytoplankton influences the biosynthetic capacities of *S. tropica* with both production of new molecules and the activation of orphan BGCs. Our work pioneers the use of phototrophs as a promising strategy to accelerate the discovery of novel natural products from actinobacteria.

Importance

The alarming increase of antimicrobial resistance has generated an enormous interest in the discovery of novel active compounds. The isolation of new microbes to untap novel natural products is currently hampered because most biosynthetic gene clusters (BGC) encoded by these microorganisms are not expressed under standard laboratory conditions, *i.e.* mono-cultures. Here we show that co-culturing can be an easy way for triggering silent BGC. By combining state-of-the-art metabolomics and high-throughput proteomics, we characterized the activation of cryptic metabolites and silent biosynthetic gene clusters in the marine actinobacteria *Salinispora tropica* by the presence of phytoplankton photosynthate. We further suggest a mechanistic understanding of the antimicrobial effect this actinobacterium has on a broad range of prokaryotic and eukaryotic phytoplankton species and reveal a promising candidate for antibiotic production.

Introduction

Soil actinomycetes are a rich source of drug-like natural products, to which we owe up to 70% of all microbial antibiotics used today (Bérdy, 2005). Identification of novel secondary metabolites from this extensively studied family has, however, stalled over the last few decades as a result of the recurring rediscovery of already known compounds. This has led in recent years to a thriving interest for the study of new microorganisms, with the rational that ecologically distinct microorganisms produce equally distinct secondary metabolites (Molinski et *al.*, 2009; Wilson and Brimble, 2009). For instance, the heterotrophic bacteria *Salinispora* drew particular attention when discovered, as it was the first obligate marine actinomycete described (Jensen *et al*., 1991; Mincer *et al*., 2002, Jensen & Mafnas, 2006) and has since proven to be an important source of new natural products for the pharmaceutical industry (Maldonado *et al.*, 2005; Feling *et al.*, 2003; Buchanan *et al*., 2005; Asolkar *et al*., 2010). Despite the increasing number of novel strains identified with promising biosynthetic capacities, many hurdles in natural product discovery remain. Most of these microbial secondary metabolites are encoded by groups of colocalized genes, called biosynthetic gene clusters (BGCs), which are now more easily identified because of the improvement in sequencing technologies and bioinformatic tools (Medema *et al*., 2011). The majority of these discovered BGCs, however, have yet to be linked to their products and are called orphan BGCs. They are generally considered to be either silent - because of a low level of expression or inactivation of their biosynthetic genes - or the metabolites they produce are cryptic - difficult to detect and isolate (Reen *et al*., 2015; Rutledge and Challis, 2015). The observation of numerous orphan BGCs in genome-sequenced microorganisms has resulted in a growing interest in developing biological or chemical means to activate such clusters (Abdelmohsen *et al*., 2015; Onaka, 2017). One of the simplest and most efficient methods described in the literature relies on co-cultivation of different microbes to elicit novel natural product biosynthesis (Slattery *et al*., 2001; Bertrand *et al*., 2014).

The genome of the marine actinomycete *Salinispora tropica* comprises at least 20 putative BGCs of which 11 are orphan (**Table 1**, Penn *et al.*, 2009, Udwary *et al*., 2007). Recent studies have shown that *Salinispora* co-inoculated with various marine heterotrophs could produce one or several antimicrobial compounds, which remain uncharacterized as traditional analytical chemistry methods did not allow their identification and no candidate BGC was proposed (Patin *et al*., 2016; Patin *et al*., 2018). While co-culturing appears to be a promising mean to activate orphan BGCs in *Salinispora*, it remains an underexplored technique to unravel the biosynthetic potential of this genus. Additionally, little has been done to establish the BGCs that are activated under such culturing conditions. Combining metabolomics with proteomics analyses has proven successful in linking novel compounds to active orphan BGCs in several *Streptomyces* species, but has not yet been applied to the genus *Salinispora* (Schley *et al*., 2006; Gubbens *et al*., 2014; Owens *et al.*, 2014).

Here we report the discovery of novel cryptic secondary metabolites produced by *S. tropica* CNB-440. By using an approach combining metabolomics and proteomics, we investigated how marine microbial phototrophs, and their photosynthate, induce the production of new metabolites and activate the expression of orphan BGCs in *S. tropica*. This strategy confirms microbial interactions as a promising and simple approach for future discovery of novel natural products.

Material and methods

1. Culture conditions and cell abundance monitoring

1.1. Strains and growth media

Axenic marine phototrophs *Synechococcus sp.* WH7803, *Emiliania huxleyi* RCC1242 and *Phaeodactylum tricornutum* CCAP1055/1 were routinely grown in Artificial Seawater (ASW, Wilson *et al*., 1996), K-media (Probert and Houdan, 2004), and F/2 media (Guillard *et al*., 1975), respectively. Cultures were set-up in Falcon 25 cm² rectangular culture flasks with vented caps containing 20 ml of media and incubated at a constant light intensity of 10 µmol photons m^{-2} s^{-1}, at 22 °C with orbital shaking (140 rpm). *Salinispora tropica* CNB-440 was grown in marine broth (MB, Difco), and incubated at 30 °C with orbital shaking (220 rpm). The *S. tropica* mutants *salA*$^-$ and *salL*$^-$ were generously provided by the Moore Laboratory, USA (Eustáquio *et al.*, 2008; Eustáquio *et al.*, 2009).

1.2. Co-culture setup

Salinispora cells were grown to late exponential phase in 10 ml of MB before washing them three times with sterile mineral media, as appropriate for each phototroph, and finally resuspending the washed cell pellet in 10 ml of mineral media. Exponentially growing axenic phototroph cells and the washed *Salinispora* were co-inoculated in fresh media to a concentration of 10% (v/v) and 20% (v/v), respectively. *Salinispora* cells were also washed and resuspended in a conditioned *Synechococcus* supernatant (SUPSYN), when required for the metabolomic and proteomic analyses. To obtain the conditioned supernatant, *Synechococcus* cultures were incubated for 35 days as described above before centrifugation (4000 x *g* for 10 min at room temperature) and further filtration through 0.22 µm pore size filters to remove cells and particulate organic matter. Washed *Salinispora* cells were used to inoculate SUPSYN and MB, and cultures were incubated at 22°C with shaking (140 rpm) and a light intensity of 10 µmol photons m^{-2} s^{-1}. For the physically separated *Synechococcus-Salinispora* co-cultures using the porous filters, cells were grown in 24 mm transwell with 0.4 µm pore polycarbonate membrane inserts (Corning). *Synechococcus* cells were inoculated in the well to a concentration of 20% (v/v) and *Salinispora* in the insert to a concentration of 55% (v/v).

1.3. Flow cytometry

Phototroph cell abundance was monitored using their autofluorescence by flow cytometry using a LSR Fortessa Flow Cytometer (BD) instrument, and the BD FACSDiva acquisition software (BD). Cells were detected and gated using ex. 488 nm – em. 710/50 nm at voltage 370 V, and ex. 640 nm – em. filter 670/14 nm at voltage 480 V. To remove any *Salinispora* cell aggregates that would block the flow cell, samples were pre-filtered through a sterile mesh with pore size of 35 µm (Corning) prior to analysis.

2. Metabolomic analysis

2.1. Sample preparation

The culture supernatants were analyzed by non-targeted metabolomic using either raw or concentrated supernatants. Raw supernatants were collected by sampling 200 µl of 0.22 µm-filtered culture milieu, prior to being mixed with an equal volume of HPLC-grade methanol. For concentrating the supernatant, cells from 10 to 100 mL of cultures were removed by centrifugation (4,000 x *g* for 15 min) followed by a filtering step using 0.22 µm vacuum filter bottle system (Corning). Pre-purification of the compounds of interest from the supernatants was carried out by solid phase extraction using C18-silica. Using a 90:10 A/B mobile phase

142 (where A is water with 0.1% formic acid and B is methanol with 0.1% formic acid) the
143 undesired polar molecules and salts passed through the silica while the compounds of interest
144 were retained and later collected following elution with a 10:90 A/B mobile phase. The
145 obtained fractions were dried under reduced pressure at 40 °C (in a speed-vac) and
146 resuspended in 1-3 mL of 50:50 HPLC-grade methanol/water solution. All samples were
147 stored in snap-seal amber glass vials (Thames Restek) and kept at -20 °C until analysis.
148
149 **2.2. Low-resolution LC-MS**
150 Metabolites present in the cultures were routinely analyzed by reversed-phase liquid
151 chromatography. A Dionex UltiMate 3000 HPLC (ThermoScientific) coupled with an amaZon
152 SL Ion Trap MS (Bruker) was used. A Zorbax Eclipse Plus C18 column with dimensions 4.6 mm
153 x 150 mm, 5 µm particle size (Agilent Technologies) was employed for metabolite separation
154 with a linear gradient of 95:5 A/B to 30:70 A/B over 5 minutes, followed by second linear
155 gradient to 20:80 A/B over 10 minutes with a flow rate of 1 ml min^{-1} (Mobile phase A: water
156 with 0.1% formic acid, B: methanol with 0.1% formic acid). The mass spectrometer was
157 operated in positive ion mode with a 100-1000 *m/z* scan range. The injected volume was 10
158 µL at a temperature of 25 °C. Data was processed with the Bruker Compass DataAnalysis
159 software version 4.2 (Bruker).
160
161 **2.3. High-resolution LC-MS**
162 To acquire molecular formulae information, samples were analyzed using an Ultra-high
163 resolution MaXis II Q-TOF mass spectrometer equipped with electrospray source coupled
164 with Dionex 3000RS UHPLC was employed (Bruker). A reverse phase C18 column (Agilent
165 Zorbax, 100x2.1 mm, 1.8 µm) and a guard column (Agilent C18, 10x2.1 mm, 1.8 µm) were
166 used for separation applying a linear gradient of 95:5 A/B to 0:100 A/B over 20 minutes
167 (Mobile phase A: water with 0.1% formic acid, B: acetonitrile with 0.1% formic acid). The
168 injected volume was 2 µL, and the flow rate was 0.2 ml min^{-1}. At the beginning of each run,
169 7.5 µl of 10 mM of sodium formate solution was injected for internal calibration. The mass
170 spectrometer was operated in positive ion mode with a 50-2500 *m/z* scan range. MS/MS data
171 was acquired for the three most intense peaks in each scan.
172
173 **3. Proteomic analysis**
174 **3.1. Preparation of cellular proteome samples**
175 Cultures were set up as described above and incubated for 5 days after which cells were
176 collected by centrifuging 10 mL of culture at 4,000 x *g* for 10 min at 4 °C. Cell pellets were
177 placed on dry ice before storing at -20 °C until further processing. The cell pellets were
178 resuspended in 200 µL 1x NuPAGE lithium dodecyl sulfate (LDS) sample buffer (ThermoFischer
179 Scientific), supplemented with 1% ß-mercaptoethanol. Cell pellets were lysed by bead beating
180 (2x45 sec and 1x30 sec at 6.0 m/s) and sonication (5 min), followed by three successive 5-min
181 incubations at 95 °C with short vortex steps in between. Cell lysates containing all proteins
182 were loaded on an SDS-PAGE precast Tris-Bis NuPAGE gel (Invitrogen), using MOPS solution
183 (Invitrogen) as the running buffer. Protein migration in the SDS-PAGE gel was performed for
184 5 min at 200 V, to allow removal of contaminants and purification of the polypeptides. The
185 resulting gel was stained using SimplyBlue SafeStain (Invitrogen) to visualize the cellular
186 proteome. The gel bands containing the cellular proteome were excised and stored at -20 °C
187 until further processing.
188

189 **3.2. Trypsin in-gel digestion and nano LC-MS/MS analysis**
190 Polyacrylamide gel bands were destained and standard in-gel reduction and alkylation were
191 performed using dithiothreitol and iodoacetamide, respectively, after which proteins were in-
192 gel digested overnight with 2.5 ng μL^{-1} trypsin (Christie-Oleza and Armengaud, 2010). The
193 resulting peptide mixture was extracted by sonication of the gel slices in a solution of 5%
194 formic acid in 25% acetonitrile, and finally concentrated at 40 °C in a speed-vac. For mass
195 spectrometry analysis, peptides were resuspended in a solution of 0.05% trifluoroacetic acid
196 in 2.5% acetonitrile prior to filtering using a 0.22 μm cellulose acetate spin column. Samples
197 were analyzed by nanoLC-ESI-MS/MS with an Ultimate 3000 LC system (Dionex-LC Packings)
198 coupled to an Orbitrap Fusion mass spectrometer (Thermo Scientific) using a 60 min LC
199 separation on a 25 cm column and settings as previously specified (Christie-Oleza *et al*., 2015).
200
201 **3.3. Proteomic data analysis**
202 Raw mass spectral files were processed for protein identification and quantification using the
203 software MaxQuant (version 1.5.5.1; Cox and Mann, 2008) and the UniProt database of *S.*
204 *tropica* CNB-440 (UP000000235). Quantification and normalization of spectral counts was
205 done using the Label-Free Quantification (LFQ) method (Cox *et al*., 2014). Samples were
206 matched between runs for peptide identification and other parameters were set by default.
207 Data processing was completed using the software Perseus (version 1.5.5.3). Proteins were
208 filtered by removing decoy and contaminants and were considered valid when present in at
209 least two replicates for one condition. The relative abundance of each protein was calculated
210 using protein intensities transformed to a logarithmic scale with base 2 and normalized to
211 protein size. Variations in protein expression were assessed with a two-sample T-test, with a
212 false discovery rate (FDR) *q* below 0.05 and a log(2) fold change above 2 (**Supplementary File**
213 **S1**).
214
215 **Results**
216 ***Salinispora tropica* has antimicrobial activity on a diverse range of marine phototrophs**
217 Unlike other heterotrophs, which usually enhance the growth of phototrophic organisms
218 when in co-culture (*e.g.* Christie-Oleza *et al*., 2017; Sher *et al*., 2011), *S. tropica* showed a clear
219 antimicrobial activity on marine phytoplankton (**Fig. 1, A**). All three phototrophic model
220 species tested, namely the cyanobacteria *Synechococcus* sp. WH7803, the coccolithophore
221 *Emiliana huxleyi* and the diatom *Phaeodactylum tricornutum*, showed a strong decline in the
222 presence of *S. tropica*, being especially remarkable for the two former species (**Fig. 1, A**).
223 While also affected, the diatom *P. tricornutum* was not killed by *S. tropica* but, instead, its
224 cells densities were significantly maintained one order of magnitude lower than when
225 incubated axenically.
226
227 We were therefore interested in characterizing the nature of this inhibition. While other
228 *Salinispora* species, such as *Salinispora arenicola*, are known to biosynthesize antibiotic
229 molecules (Asolkar *et al*., 2010), no antimicrobial compound has yet been characterized in *S.*
230 *tropica* CNB-440. Previous studies have shown, however, that *S. tropica* is able to outcompete
231 other heterotrophs in co-culture by secreting siderophores leading to iron depletion (Patin *et*
232 *al.*, 2016). To evaluate whether iron sequestration could explain the negative interactions
233 observed in the present phototroph-*Salinispora* system, we supplemented the co-cultures
234 with increasing concentrations of iron (**Supplementary Fig. S1**). The results obtained suggest

235 that the antimicrobial phenotype was not due to siderophore activity, as saturating amount
236 of iron could not rescue the growth of the phototrophs.
237
238 We then hypothesized that a yet unknown antimicrobial compound, to which our
239 photosynthetic microorganisms are sensitive to, could be produced by *S. tropica.* To test this
240 assumption, we setup co-cultures in which *S. tropica* and *Synechococcus* were physically
241 separated by a porous filter, preventing direct cell-to-cell interactions while allowing the
242 diffusion of small molecules (**Fig. 1, B**). *S. tropica* was still able to impair *Synechococcus*
243 proliferation in these experimental conditions, confirming that a secreted molecule was
244 causing the death of the phototroph.
245
246 **Phototrophs elicit the production of novel cryptic metabolites in *S. tropica***
247 We analyzed the co-culture supernatants using non-targeted metabolomics to identify the
248 pool of secondary metabolites secreted by *S. tropica* in response to the different phototrophs.
249 The *Synechococcus-S. tropica* co-culture revealed eight molecular ions that were not present
250 in the respective axenic cultures (**Fig. 2, A**). These molecules were further characterized by
251 high-resolution MS/MS analysis, from which we generated empirical chemical formulae,
252 allowing us to assign most of them to two subgroups of related compounds being: (i) ions **1**,
253 **2**, **5** and **8**; and (ii) ions **4**, **6** and **7** (**Fig. 2, A** and **Supplementary Table S1**).
254
255 Ions **1**, **2**, **5** and **8** were derivatives of salinosporamide; a well-characterized molecule
256 produced by *S. tropica* that presents a unique fused γ-lactam-β-lactone bicyclic ring structure
257 (Feling *et al*., 2003), and that is now being tested as a drug because of its anti-cancer
258 properties. Molecules **5** and **8** are consistent with known degradation products of
259 salinosporamide A and B, respectively (Denora *et al*., 2007; **Supplementary Fig. S2**), while
260 molecules **1** and **2** are proposed to result from the nucleophilic addition of Tris (the buffering
261 agent used in the ASW culture medium) to the lactone ring of salinosporamide A and B,
262 respectively (**Supplementary Fig. S2**). These salinosporamide sub-products were further
263 confirmed by their absence when i) Tris was not added (**Supplementary Fig. S3**), or ii)
264 salinosporamide mutants that no longer produced these metabolites, *i.e.* salA$^-$ and salL$^-$
265 (Eustáquio *et al*., 2009), were used (**Supplementary Fig. S4**). In order to test the activity of
266 salinosporamide and its derivatives on the phototrophs, we co-cultured *Synechococcus* with
267 both salinosporamide mutants. Salinosporamide and its derivatives were not responsible for
268 the antimicrobial activity as both deficient mutants were still able to inhibit the phototroph
269 (**Supplementary Fig. S5**).
270
271 The second group of ions, *i.e.* peaks **4**, **6** and **7**, were also related. Molecule **6** gave a *m/z* value
272 of 435.2609 $[M+H]^+$; based on the accuracy of this value and the isotopic pattern the empirical
273 chemical formula $C_{22}H_{35}N_4O_5$ was predicted by the DataAnalysis software (**Table 2**). The
274 predicted formula for molecule **4** suggests that, with a 28.9900 Da mass difference when
275 compared to **6**, the compound had lost one hydrogen and gained an atom of nitrogen and
276 oxygen. MS/MS analyses confirmed that both molecules **4** and **6** had an identical molecular
277 fragment (*i.e. m/z* 276.1600 ± 0.0001 $[M+H]^+$, with the empirical chemical formula
278 $C_{16}H_{22}NO_3$), indicating that the two molecules share a core backbone (**Table 2**). Similarly,
279 molecule **7** had the same chemical formula than **6** but with the addition of a methyl group
280 (14.0155 Da mass difference; **Table 2**). Molecule **3** did not share an obvious link to any other
281 metabolites and, therefore, was considered a new biosynthesized product of *Salinispora*

282 (**Table 2**). Most interestingly, the search for compounds with the same molecular formulae as
283 **3**, **4**, **6** or **7** in multiple databases (*e.g.* Reaxys, SciFinder, Dictionary of NP) returned no known
284 natural product, suggesting that they are novel compounds. Unfortunately, despite multiple
285 attempts, the isolation of these molecules has so far proven too challenging for their
286 structural elucidation.
287
288 The production of these novel compounds was only triggered by the presence of the
289 phototrophs as they were only detected in the co-cultures of all three phototrophs (**Fig. 2, A**
290 **and B**), but not when grown in mono culture – as shown by the absence of these metabolites
291 when *S. tropica* was grown alone in mineral ASW or nutrient rich media MB (**Fig. 2, C and D**).
292 Furthermore, we confirmed that the supernatant of a phototroph culture – containing the
293 photosynthate – was enough to induce such metabolite production (**Fig. 2, D**).
294
295 **Photosynthate triggers the expression of orphan gene clusters in *S. tropica***
296 Having detected novel secondary metabolites produced by *S. tropica* in response to
297 phototroph-released photosynthate, we set out to investigate how it affected the induction
298 of its BGCs. To this end, we analyzed and compared the proteome of *S. tropica* when grown
299 in presence of the phytoplankton's photosynthate – *i.e.* in conditioned *Synechococcus*
300 supernatant – and in nutrient rich broth – *i.e.* marine broth. Surprisingly, we were able to
301 detect proteins encoded by almost all of *S. tropica*'s BGCs, including 10 of its 11 orphans BGCs
302 (**Fig. 3, A**).
303
304 Of particular interest were the orphan BGCs *pks3* and *nrps1*, for which we detected 72%
305 (18/25) and 42% (14/33) of their encoded proteins, respectively (**Fig. 3, A**). Moreover, the
306 *pks3* BGC was noticeably highly detected as eight of its detected proteins showed a relative
307 abundance above 0.1% (**Supplementary Table S2**). While it has been previously suggested
308 that *pks3* may produce a spore pigment polyketide, very little experimental evidence is
309 available in the literature, and the product of *pks3* had not been confirmed (Kersten *et al*.,
310 2013). On the other hand, the non-ribosomal peptide synthetase (NRPS) gene cluster *nrps1*
311 has only been predicted to produce a non-ribosomal dipeptide (Penn *et al*., 2009).
312 Intriguingly, the most abundant proteins detected from this *nrps1* BGC were the non-
313 ribosomal peptide synthetase (A4X2Q0), the condensation domain-containing protein
314 (A4X2R5) and an ATP-dependent Clp protease subunit (A4X2S2), with a relative abundance of
315 0.004%, 0.001% and 0.121%, respectively (**Table 3**). While the two former are thought to
316 direct the biosynthesis of the non-ribosomal peptide, the later may be involved in conferring
317 resistance to the synthesized antimicrobial compound (Kirstein *et al.*, 2009), as further
318 discussed below.
319
320 The already characterized *lom* and *sal* BGCs were also abundantly detected with 81% (47/58)
321 and 77% (23/30) of their encoded proteins detected, respectively, some representing high
322 relative abundances within the proteome (**Fig. 3, A**). The BGC *lom* is linked to the cytotoxic
323 glycoside lomaiviticin molecule (Kersten *et al*., 2013). However, this metabolite previously
324 showed no antimicrobial activity on co-cultured heterotrophic organisms (Patin *et al.*, 2018)
325 and, hence, it is unlikely to cause the antimicrobial phenotype observed on the phototrophs
326 in this study. The high abundance of the *sal* cluster, producing the salinosporamide
327 compound, is not surprising given the high detection of this metabolite by LC-MS (**Fig. 2, A**).
328

329 Interestingly, the comparative proteomic analysis of *S. tropica* grown in photosynthate *versus*
330 marine broth confirmed that the detection of several BGCs rose in response to phototroph-
331 released nutrients, being *lom* and *pks3* the most remarkable ones (**Fig. 3, B-C**). For instance,
332 the *lom* cluster had 77% (36/47) of its detected proteins overexpressed in the presence of the
333 photosynthate (**Fig. 3, B**). The orphan *pks3* BGC was also triggered by the photosynthate, as
334 the pivotal biosynthetic enzymes for polyketide biosynthesis, *i.e.* acyl-CoA ligase (A4X7T8), 3-
335 ketoacyl-ACP synthase (A4X7U0) and long-chain fatty acid-CoA ligase (A4X7U3), were up-
336 regulated (3.1, 2.6 and 4.1-fold change, respectively; **Fig. 3, C** and **Supplementary Table S2**).
337
338 **Discussion**
339 We show that *S. tropica* is able to inhibit the growth of both marine cyanobacteria and
340 eukaryotic phototrophs by some, yet, unidentified mechanism (**Fig. 1**). This observation
341 broadens the potential role and impact that the *Salinispora* genus has on marine microbial
342 communities. *Salinispora* is a widely-distributed bacterium found in all tropical and
343 subtropical oceans (Mincer *et al*., 2002; Bauermeister *et al*., 2018). While mostly inhabiting
344 marine sediments, bacteria from this genus were also isolated from marine sponges where it
345 is suggested they influence the sponge microbiota through the production of acyl homoserine
346 lactone molecules and antibiotics (Singh *et al*., 2014; Bose *et al*., 2017). Similarly, different
347 species of *Salinispora* were shown to possess distinct mechanisms to outcompete co-
348 occurring marine heterotrophs in sediments, *i.e.* through the production of siderophores to
349 deplete iron or antimicrobial molecules (Patin *et al*., 2017; Tuttle *et al*., 2019), although no
350 antimicrobial compound has yet been identified for *S. tropica* (Patin *et al.*, 2018). We herein
351 provide the first evidence that *Salinispora* might not only directly influence heterotrophic
352 communities, but also kill both prokaryotic and eukaryotic phytoplankton to which they are
353 exposed, *e.g.* when these sediment out of the water column or phototrophs able to grow in
354 sunlit coastal sediments.
355
356 While we were successful in identifying and obtaining the molecular formulae of novel cryptic
357 metabolites produced in response to phytoplanktonic photosynthate (**Fig. 2**, **Table 2**), we
358 were unable to isolate and identify the compound responsible for the antimicrobial effect on
359 the marine phototrophs by using traditional bioactivity-guided assays with HPLC fractionation
360 of crude extracts (data not shown). This mechanism proved similarly elusive in previous
361 studies, where *S. tropica* showed an antimicrobial activity on marine heterotrophs, but the
362 molecule responsible was not identified (Patin *et al*., 2016; Patin *et al*., 2018). The parallelism
363 between our observations and those described in the literature suggests that the active
364 compound(s) may be the same. We reason that the compound's instability, and/or synergic
365 effect of several molecules required for activity, could explain the difficulty in identifying the
366 antimicrobial agent. For instance, the large number of structurally-related metabolites
367 resulting from the chemical reaction of salinosporamide with various compounds (*i.e*. water,
368 Tris) may support this hypothesis, as the antimicrobial molecule may be similarly unstable.
369 The diversity of products arising from a single BGC may also be due to the promiscuity of the
370 biosynthetic enzymes utilizing structurally related primary precursors. This results in a range
371 of compounds, each produced at lower titers than a single natural product, and ultimately
372 hamper the isolation of sufficient amounts of the compounds of interest. Whichever the case,
373 we show that *Salinispora* can produce a broad-range antibiotic able to affect both unicellular
374 prokaryotes and eukaryotes alike, such as the marine diatom and coccolithophore tested in
375 our study. Such a broad-range antimicrobial could suggest a mode of action affecting a

376 common target present in both types of cells such as the proteasome, a proteolytic complex
377 present in the three domains of life (Becker and Darwin, 2016).
378
379 Exploring the proteome of *S. tropica* exposed to photosynthate, we detected proteins
380 encoded by almost all its BGCs, including most of its orphan BGCs (**Fig. 3**). Notably, the *sal*
381 BGC, producing the salinosporamide compound, was one of the most highly expressed BGC
382 as most of its proteins were detected with high relative abundance. This finding is in
383 agreement with previous studies that have shown by transcriptomics that the BGC *sal* is highly
384 and constitutively expressed when grown in nutrient rich A1 medium (Amos *et al*., 2017).
385 Also, the high expression of this BGC correlated with a noticeable detection of
386 salinosporamide derivatives by LC-MS. The agreement between the metabolomic and
387 proteomic data suggests that it is possible to correlate activated BGCs with the actual
388 biosynthesis of their corresponding natural product. Therefore, the abundant detection of
389 several orphans BGC proteins, including those from *pks3* and *nrps1* BGCs, may be promising
390 candidates responsible for the biosynthesis of the cryptic metabolites detected by LC-MS and,
391 potentially, the antimicrobial activity observed on co-cultured phototrophs.
392
393 The proteins detected from the BGC *nrps1* are essential enzymes involved in non-ribosomal
394 peptide biosynthesis, *i.e.* A4X2Q0, a non-ribosomal peptide synthetase (NRPS) made of a C-
395 A-PCP domain, and A4X2RS, a condensation domain-containing protein made of C-PCP-TE
396 domain. The detection of these proteins therefore strongly suggests the actual synthesis of
397 the non-ribosomal peptide and could well be the novel metabolites detected by LC-MS, which
398 include four nitrogen atoms in their predicted molecular formulae (**Table 2**). Interestingly, the
399 substrate specificity of A4X2Q0's A-domain is alanine and another three A-domains are
400 encoded in the *nrps1* BGC. Further work is required to elucidate the structure of this series of
401 cryptic metabolites. From this same BGC we also detected a highly abundant ATP-dependent
402 Clp protease proteolytic subunit (ClpP, A4X2S2) that may be providing *Salinispora* with self-
403 resistance against the *nrps1* peptides. Virtually all organisms across the tree of life have a
404 system for targeted proteolysis for protein turnover, with most bacteria, mitochondria and
405 chloroplasts relying on a ClpP-type proteasome while eukaryotes, archaea and some
406 actinobacteria typically possess the homologous 20S proteasome structure (Becker and
407 Darwin, 2016; Snoberger *et al*., 2017). The ClpP proteasome is known to be the target for
408 certain antibiotics, including the novel acyldepsipeptide (ADEP) class (Kirstein *et al.*, 2009),
409 and it is common to find alternative ClpP proteasomes encoded nearby the antibiotic-
410 producing BGC to confer resistance to the host cell (Thomy *et al*., 2019). In a similar fashion,
411 salinosporamide A is a 20S proteasome inhibitor, to which *Salinispora* is resistant because of
412 an extra copy of the proteasome beta subunit gene within the salinosporamide-producing
413 cluster (Kale *et al*., 2011). We can thus reasonably infer from the presence of *clpP* in the *nrps1*
414 BGC that it is likely to produce an antibiotic targeting the ClpP proteasome, a class of
415 antimicrobial compounds that has recently gained considerable attention as an attractive
416 option to tackle multidrug resistant pathogens (**Fig. 4**; Momose and Kawada, 2016; Culp and
417 Wright, 2017; Moreno-Cinos *et al.*, 2019). We here provide the first proteomic evidence that
418 *S. tropica*'s *nrps1* is active and may produce a promising antimicrobial compound acting as a
419 ClpP proteasome inhibitor. The synthesis of such antibiotic would explain the antimicrobial
420 effect of *Salinispora* on all marine phototrophs tested in our study as they all rely on the ClpP
421 proteolytic machinery (Andersson *et al.*, 2009; Jones *et al.*, 2013; Zhao *et al.*, 2018). Additional
422 evidence, such as genetic inactivation of the *nrps1* BGC, will confirm this mechanism.

We show that the photosynthate released by primary producers influences the biosynthetic capacities of *Salinispora*, activating the expression of several orphan BGCs and inducing the production of novel metabolites. Our metabolomics analysis further confirmed the potential of co-culturing for natural product discovery as we identified novel cryptic secondary metabolites, although future work is required to elucidate the structure of the new molecules. Finally, our study extends the pool of known compounds produced by the genus *Salinispora* and pioneers the use of phototrophs as a promising strategy to trigger novel natural products from marine actinobacteria. We also provide a valuable insight into the biosynthetic potential of *S. tropica* with our proteomic dataset, which reveals the *nrps1* BGC as a promising candidate for antibiotic production.

Conflicts of interest

The authors declare that they have no conflicts of interest.

Acknowledgments

We thank Vinko Zadjelovic, Linda Westermann and Fabrizio Alberti for helpful discussions throughout the project. We also acknowledge technical support from Cleidiane Zampronio of the WPH Proteomic Facility at the University of Warwick. In addition, we thank the BBSRC/EPSRC Synthetic Biology Research Centre WISB BB/M017982/1 for access to the flow cytometer and Yin Chen for access to the LC-MS.

A.C. was supported by an MIBTP PhD scholarship (BB/M01116X/1) and D.S. by a NERC CENTA DTP studentship (NE/L002493/1). J.A.C.-O was funded by a NERC Independent Research Fellowship NE/K009044/1 and Ramón y Cajal contract RYC-2017-22452 (funded by the Ministry of Science, Innovation and Universities, the National Agency of Research, and the European Social Fund). C.C. thanks BBSRC (grant BB/M022765/1) and European Union's Horizon 2020 research No. 765147 for support. L.S. would like to acknowledge BBSRC (BB/M017982/1 and BB/R000689/1) and EPSRC (EP/P0305721/1) for financial support.

References

Abdelmohsen UR, Grkoviv T, Balasubramanian S, Kamel MS, Quinn RJ, Hentschel U: **Elicitation of secondary metabolism in actinomycetes.** *Biotechnol Adv* (2015), 33(6 Pt 1):798-811. doi: 10.1016/j.biotechadv.2015.06.003.

Andersson FI, Tryggvesson A, Sharon M, Diemand AV, Classen M, Best C, Schmidt R, Schelin J, Stanne TM, Bukau B, Robinson CV, Witt S, Mogk A, Clarke AK: **Structure and function of a novel type of ATP-dependent Clp protease.** *J Biol Chem* (2009), 284(20):13519-32. doi: 10.1074/jbc.M809588200.

Asolkar RN, Kirkland TN, Jensen PR, Fenical W: **Arenimycin, an antibiotic effective again rifampin- and methicillin-resistant *Staphylococcus aureus* from the marine actinomycete *Salinispora arenicola***. *J Antibio* (2010), 63(1):37-0. doi: 10.1038/ja.2009.114.

469 Bauermeister A, Velasco-Alzate K, Dias T, Macedo H, Ferreira EG, Jimenez PC, Lotufo TMC,
470 Lopes NP, Gaudêncio SP, Costa-Lotufo LV: **Metabolomic fingerprinting of Salinispora from**
471 **Atlantic oceanic islands**. *Front Microbiol* (2018), 9:3021. doi: 10.3389/fmicb.2018.03021.
472
473 Becker SH, Darwin KH: **Bacterial proteasomes: mechanistic and functional insights.** *Microbiol*
474 *Mol Biol Rev* (2016), 81(1). doi: 10.1128/MMBR.00036-16.
475
476 Bérdy J: **Bioactive microbial metabolites**. *J Antibiot* (2005), 58(1):1-26. doi:
477 10.1038/ja.2005.1.
478
479 Bertrand S, Bohni N, Schnee S, Schumpp O, Gindro K, Wolfender JL: **Metabolite induction via**
480 **microorganism co-culture: a potential way to enhance chemical diversity for drug discovery**.
481 *Biotechnol Adv* (2014), 32(6):1180-204. doi: 10.1016/j.biotechadv.2014.03.001.
482
483 Bose U, Ortori CA, Sarmad S, Barrett DA, Hewavitharana AK, Hodson MP, Fuerst JA, Shaw PN,
484 Boden R: **Production of N-acyl homoserine lactones by the sponge-associated marine**
485 **actinobacteria *Salinispora arenicola* and *Salinispora pacifica*.** FEMS Microbiol Lett (2017),
486 364(2). doi: 10.1093/femsle/fnx002.
487
488 Buchanan GO, Williams PG, Feling RH, Kauffman CA, Jensen PR, Fenical W: **Sporolides A and**
489 **B: structurally unprecedented halogenated macrolides from the marine actinomycete**
490 ***Salinispora tropica*.** *Org Lett* (2005), 7(13):2731-4. doi: 10.1021/ol050901i.
491
492 Christie-Oleza JA, Armengaud J: **In-depth analysis of exoproteomes from marine bacteria by**
493 **shotgun liquid chromatography-tandem mass spectrometry: the *Ruegeria pomeroyi* DSS-3**
494 **case-study.** *Mar Drugs* (2010), 8(8):2223-39. doi: 10.3390/md8082223.
495
496 Christie-Oleza JA, Scanlan DJ, Armengaud J: **"You produce while I clean up", a strategy**
497 **revealed by exoproteomics during Synechococcus-Roseobacter interactions.** *Proteomics*
498 (2015), 15(20):3454-62. doi: 10.1002/pmic.201400562.
499
500 Christie-Oleza JA, Sousoni D, Lloyd M, Armengaud J, Scanlan DJ: **Nutrient recycling facilitates**
501 **long-term stability of marine microbial phototroph-heterotroph interactions.** *Nat Microbiol*
502 (2017), 2:17100. doi: 10.1038/nmicrobiol.2017.100.
503
504 Cox J, Hein MY, Luber CA, Paron I, Nagaraj N, Mann M: **Accurate proteome-wide label-free**
505 **quantification by delayed normalization and maximal peptide ratio extraction, termed**
506 **MaxLFQ.** *Mol Cell Proteomics* (2014), 13(9):2513-26. doi: 10.1074/mcp.M113.031591.
507
508 Cox J, Mann M: **MaxQuant enables high peptide identification rates, individualized p.p.b.-**
509 **range mass accuracies and proteome-wide protein quantification.** *Nat Biotechnol* (2008),
510 26(12):1367-72. doi: 10.1038/nbt.1511.
511
512 Culp E, Wright GD: **Bacterial proteases, untapped antimicrobial drug targets.** *J Antibiot*
513 *(Tokyo)* (2017), 70(4):366-377. doi: 10.1038/ja.2016.138.
514

515 Denora N, Potts BC, Stella VJ: **A mechanistic and kinetic study of the beta-lactone hydrolysis**
516 **of Salinosporamide A (NPI-0052), a novel proteasome inhibitor.** *J Pharm Sci* (2007),
517 96(8):2037-47. doi: 10.1002/jps.20835.
518
519 Dineshkumar K, Aparna V, Madhuri KZ, Hopper W: **Biological activity of sporolides A and B**
520 **from Salinispora tropica: in silico target prediction using ligand-based pharmacophore**
521 **mapping and in vitro activity validation on HIV-1 reverse transcriptase.** *Chem Biol Drug Des*
522 (2014), 83(3):350-61. doi: 10.1111/cbdd.12252.
523
524 Eustáquio AS, McGlinchey RP, Liu Y, Hazzard C, Beer LL, Florova G, Alhamadsheh MM, Lechner
525 A, Kale AJ, Kobayashi Y, Reynolds KA, Moore BS: **Biosynthesis of the salinosporamide A**
526 **polyketide synthase substrate chloroethylmalonyl-coenzyme A from S-adenosyl-L-**
527 **methionine**. *Proc Natl Acad Sci USA* (2009), 106(30):12295-300. doi:
528 10.1073/pnas.0901237106.
529
530 Eustáquio AS, Pojer F, Noel JP, Moore BS: **Discovery and characterization of a marine**
531 **bacterial SAM-dependent chlorinase**. *Nat Chem Biol* (2008), 4(1):69-74. doi:
532 10.1038/nchembio.2007.56.
533
534 Feling RH, Buchanan GO, Mincer TJ, Kauffman CA, Jensen PR, Fenical W: **Salinosporamide A:**
535 **a highly cytotoxic proteasome inhibitor from a novel microbial source, a marine bacterium**
536 **of the new genus Salinospora**. *Angew Chem Int Ed Engl* (2003), 42(3):355-7. doi:
537 10.1002/anie.200390115.
538
539 Guillard RRL: **Culture of phytoplankton for feeding marine invertebrates.** In: Smith W.L.,
540 Chanley M.H. (eds) *Culture of Marine Invertebrate Animals. Springer, Boston, MA* (1975), 29-
541 60. doi: https://doi.org/10.1007/978-1-4615-8714-9_3.
542
543 Gubbens J, Zhu H, Girard G, Song L, Florea BI, Aston P, Ichinose K, Filippov DV, Choi YH,
544 Overkleeft HS, Challis GL, van Wezel GP: **Natural product proteomining, a quantitative**
545 **proteomics platform, allows rapid discovery of biosynthetic gene clusters for different**
546 **classes of natural products**. *Chem Biol* (2014). 21(6):707-18. doi:
547 10.1016/j.chembiol.2014.03.011.
548
549 Jensen PR, Dwight R, Fenical W: **Distribution of actinomycetes in near-shore tropical marine**
550 **sediments.** *Appl Environ Microbiol* (1991), 57(4):1102-8
551
552 Jensen PR, Mafnas C: **Biogeography of the marine actinomycete Salinispora.** *Environ*
553 *Microbiol* (2006), 8(11):1881-8. doi: 10.1111/j.1462-2920.2006.01093.x.
554
555 Jones BM, Iglesias-Rodriguez MD, Skipp PJ, Edwards RJ, Greaves MJ, Young JR, Elderfield H,
556 O'Connor CD: **Responses of the Emiliania huxleyi proteome to ocean acidification.** *PLoS One*
557 (2013), 8(4). doi: 10.1371/journal.pone.0061868.
558
559 Kale AJ, McGlinchey RP, Lechner A, Moore BS: **Bacterial self-resistance to the natural**
560 **proteasome inhibitor salinosporamide A.** *ACS Chem Biol* (2011), 6(11):1257-64. doi:
561 10.1021/cb2002544.

562
563 Kersten RD, Lane AL, Nett M, Richter TKS, Duggan BM, Dorrestein PC, Moore BS: **Bioactivity-**
564 **guided genome mining reveals the lomaiviticin biosynthetic gene cluster in *Salinispora***
565 ***tropica*.** *ChemBioChem* (2013). 14:955-962. doi: 10.1002/cbic.201300147.
566
567 Kirstein J, Hoffmann A, Lilie H, Schmidt R, Rübsamen-Waigmann H, Brötz-Oesterhelt H, Mogk
568 A, Turgay K: **The antibiotic ADEP reprogrammes ClpP, switching it from a regulated to an**
569 **uncontrolled protease.** *EMBO Mol Med* (2009), 1(1):37-49. doi: 10.1002/emmm.200900002.
570
571 Maldonado LA, Fenical W, Jensen PR, Kauffman CA, Mincer TJ, Ward AC, Bull AT, Goodfellow
572 M: ***Salinispora arenicola* gen. nov., sp. nov. and *Salinispora tropica* sp. nov., obligate marine**
573 **actinomycetes belonging to the family Micromonosporaceae**. *Int J Syst Evol Microbiol*
574 (2005), 55(Pt 5):1759-66. doi: 10.1099/ijs.0.63625-0.
575
576 Medema MH, Blin K, Cimermancic P, de Jager V, Zakrzewski P, Fischbach MA, Weber T, Takano
577 E, Breitling R: **antiSMASH: rapid identification, annotation and analysis of secondary**
578 **metabolite biosynthesis gene clusters in bacterial and fungal genome sequences.** *Nucleic*
579 *Acids Res* (2011). 39:W339-46. doi: 10.1093/nar/gkr466.
580
581 Miyanaga A, Janso JE, McDonarld L, He M, Liu H, Barbieri L, Eustáquio AS, Fielding EN, Carter
582 GT, Jensen PR, Feng X, Leighton M, Koehn FE, Moore BS: **Discovery and Assembly Line**
583 **Biosynthesis of the Lymphostin Pyrroloquinoline Alkaloid Family of mTOR Inhibitors in**
584 **Salinispora Bacteria.** *J Am Chem Soc* (2011), 133(34):13311-13313. doi: 10.1021/ja205655w.
585
586 Mincer TJ, Jensen PR, Kauffman CA, Fenical W: **Widespread and persistent populations of a**
587 **major new marine actinomycete taxon in ocean sediments.** *Appl Environ Microbiol* (2002),
588 68(10):5005-11. doi: 10.1128/aem.68.10.5005-5011.2002.
589
590 Molinski TF, Dalisay DS, Lievens SL, Saludes JP: **Drug development from marine natural**
591 **products.** *Nat Rev Drug Discov* (2009), 8(1):69:85. doi: 10.1038/nrd2487.
592
593 Momose I, Kawada M: **The therapeutic potential of microbial proteasome inhibitors.** *Int*
594 *Immunopharmacol* (2016), 37:23-30. doi: 10.1016/j.intimp.2015.11.013.
595
596 Moreno-Cinos C, Goossens K, Salado IG, Van Der Veken P, De Winter H, Augustyns K: **ClpP**
597 **protease, a promising antimicrobial target.** *Int J Mol Sci* (2019), 20(9). doi:
598 10.3390/ijms20092232.
599
600 Onaka H: **Novel antibiotic screening methods to awaken silent or cryptic secondary**
601 **metabolic pathways in actinomycetes.** *J Antibio* (2017), 70(8):865-870. doi:
602 10.1038/ja.2017.51.
603
604 Owens RA, Hammel S, Sheridan KJ, Jones GW, Doyle S: **A proteomic approach to investigating**
605 **gene cluster expression and secondary metabolite functionality in *Aspergillus fumigatus*.**
606 *PLoS One* (2014), 9(9):e106942. doi: 10.1371/journal.pone.0106942.
607

608 Patin NV, Duncan KR, Dorrestein PC, Jensen PR: **Competitive strategies differentiate closely**
609 **related species of marine actinobacteria.** *ISME J* (2016), 10(2):478-90. doi:
610 10.1038/ismej.2015.128.
611
612 Patin NV, Floros DJ, Hughes CC, Dorrestein PC, Jensen PR: **The role of inter-species**
613 **interactions in Salinispora specialized metabolism.** *Microbiology* (2018), 164(7):946-955.
614 doi: 10.1099/mic.0.000679.
615
616 Patin NV, Schorn M, Aguinaldo K, Lincecum T, Moore BS, Jensen PR: **Effects of Actinomycetes**
617 **secondary metabolites on sediment microbial communities.** *Appl Environ Microbiol* (2017),
618 83(4). doi: 10.1128/AEM.02676-16.
619
620 Penn K, Jenkins C, Nett M, Udwary DW, Gontang EA, McGlinchey Rp, Foster B, Lapidus A,
621 Podell S, Allen EE, Moore BS, Jensen PR: **Genomic islands link secondary metabolism to**
622 **functional adaptation in marine Actinobacteria**. *ISME J* (2009), 3(10):1193-203. doi:
623 10.1038/ismej.2009.58.
624
625 Probert I, Houdan A: **The Laboratory Culture of Coccolithophores.** In: Thierstein H.R., Young
626 J.R. (eds) *Coccolithophores. Springer, Berlin, Heidelberg* (2004). doi:
627 https://doi.org/10.1007/978-3-662-06278-4_9.
628
629 Reen FJ, Romano S, Dobson ADW, O'Gara F: **The sound of silence: activating silent**
630 **biosynthetic gene clusters in marine microorganisms**. *Mar Drugs* (2015), 13(8):4754-4783.
631 10.3390/md13084754.
632
633 Richter TKS, Hughes CC, Moore BS: **Sioxanthin, a novel glycosylated carotenoid reveals an**
634 **unusual subclustered biosynthetic pathway.** *Environ Microbiol* (2015), 17(6):2158-2171. doi:
635 10.1111/1462-2920.12669.
636
637 Roberts AA, Schultz AW, Kersten RD, Dorrestein PC, Moore BS: **Iron acquisition in the marine**
638 **actinomycete genus Salinispora is controlled by the desferrioxamine family of**
639 **siderophores.** *FEMS Microbiol Lett* (2012), 335(2):95-103. doi: 10.1111/j.1574-
640 6968.2012.02641.x.
641
642 Rutledge PJ, Challis GL: **Discovery of microbial natural products by activation of silent**
643 **biosynthetic gene clusters**. *Nat Rev Microbiol* (2015), 13(8):509-23. doi:
644 10.1038/nrmicro3496.
645
646 Schley C, Altmeyer MO, Swart R, Müller R, Huber CG: **Proteome analysis of *Myxococcus***
647 ***xanthus* by off-line two-dimensional chromatographic separation using monolithic poly-**
648 **(styrene-divinylbenzene) columns combined with ion-trap tandem mass spectrometry**. *J*
649 *Proteome Res* (2006), 5(10):2760-8. doi: 10.1021/pr0602489.
650
651 Sher D, Thompson JW, Kashtan N, Croal L, Chisholm SW: **Response of *Prochlorococcus***
652 **ecotypes to co-culture with diverse marine bacteria.** *ISME J* (2011), 5(7):1125-32. doi:
653 10.1038/ismej.2011.1.
654

655 Singh S, Prasad P, Subramani R, Aalbersberg W: **Production and purification of a bioactive**
656 **substance against multi-drug resistant human pathogens from the marine-sponge-derived**
657 ***Salinispora* sp.** *Asian Pac J Trop Biomed* (2014), 4(10):825-831. doi:
658 10.12980/APJTB.4.2014C1154.
659
660 Slattery M, Rajbhandari I, Wesson K: **Competition-mediated antibiotic induction in the**
661 **marine bacterium *Streptomyces tenjimariensis*.** *Microb Ecol* (2001), 41(2);90-96. doi:
662 10.1007/s002480000084.
663
664 Snoberger A, Anderson RT, Smith DM: **The proteasomal ATPases use a slow but highly**
665 **processive strategy to unfold proteins.** *Front Mol Biosci* (2017). 4:18. doi:
666 10.3389/fmolb.2017.00018.
667
668 Süssmuth RD, Mainz A: **Nonribosomal peptide synthesis-principles and prospects.** *Angew*
669 *Chem Int Ed Engl* (2017), 56(14):3770-3821. doi: 10.1002/anie.201609079.
670
671 Thomy D, Culp E, Adamek M, Cheng EY, Ziemert N, Wright GD, Sass P, Brötz-Oesterhelt H: **The**
672 **ADEP biosynthetic gene cluster in *Streptomyces hawaiiensis* NRRL 15010 reveals an**
673 **accessory *ClpP* gene as a novel antibiotic resistance factor.** *Appl Environ Microbiol* (2019),
674 85(20). doi: 10.1128/AEM.01292-19.
675
676 Tuttle NR, Demko AM, Patin NV, Kapono CA, Donia MS, Dorrestein P, Jensen PR: **Detection of**
677 **natural products and their producers in ocean sediments.** *Appl Environ Microbiol* (2019),
678 85(8). doi: 10.1128/AEM.02830-18.
679
680 Udwary DW, Zeigler L, Asolkar RN, Singan V, Lapidus A, Fenical W, Jensen PR, Moore BS:
681 **Genome sequencing reveals complex secondary metabolome in the marine actinomycete**
682 ***Salinispora tropica***. *Proc Natl Acad Sci USA* (2007), 104(25);10376-81. doi:
683 10.1073/pnas.0700962104.
684
685 Wilson WH, Carr NG, Mann NH: **The effect of phosphate status on the kinetics of cyanophage**
686 **infection in the oceanic cyanobacterium *Synechococcus* sp. WH7803**. *J Phycol* (1996), 32(4).
687 doi: 10.1111/j.0022-3646.1996.00506.x.
688
689 Wilson ZE, Brimble MA: **Molecules derived from the extremes of life.** *Nat Prod Rep* (2009),
690 26(1):44-71. doi: 10.1039/b800164m.
691
692 Zhao P, Gu W, Huang A, Wu S, Liu C, Huan L, Gao S, Xie X, Wang G: **Effect of iron on the growth**
693 **of *Phaeodactylum tricornutum* via photosynthesis.** *J phycol* (2018), 54(1):34-43. doi:
694 10.1111/jpy.12607.
695

Table 1 | Biosynthetic gene clusters of *Salinispora tropica* CNB-440. Table shows the characterized (in orange) and orphan (in green) BGCs of *S. tropica* CNB-440.

BGC name	Biosynthetic class	Product	Genetic location (strop_)	Size (kb)	Reference
sal	polyketide/non-ribosomal peptide	salinosporamide	RS05130-RS05275	41.8	Feling *et al.*, 2003
lom	polyketide	lomaiviticin	RS10930-RS11215	62.2	Kersten *et al.*, 2013
des	hydroxamate	desferrioxamine	RS12775-RS12855	19.2	Roberts *et al.*, 2012
spo	polyketide	sporolide	RS13560-RS13730	49.2	Dineshkumar *et al.*, 2014
slm	polyketide	salinilactam	RS13850-RS13965	82.0	Udwary *et al.*, 2007
lym	polyketide/non-ribosomal peptide	lymphostin	RS15295-RS15350	25.0	Miyanaga *et al.*, 2011
terp1	terpenoid	sioxanthin	RS16250-RS16295	10.4	Richter *et al.*, 2015
spt	butyrolactone	salinipostin	RS20900-RS20940	11.1	Amos *et al.*, 2017
terp2	terpenoid	sioxanthin	RS22405-RS22445	11.7	Richter *et al.*, 2015
pks1	polyketide	*NA*	RS02980-RS03095	30.9	*NA*
nrps1	non-ribosomal peptide	*NA*	RS03375-RS03535	37.5	*NA*
amc	carbohydrate	*NA*	RS11765-RS11795	6.6	*NA*
bac1	ribosomal peptide	*NA*	RS11800-RS12275	19.2	*NA*
pks3	polyketide	*NA*	RS12510-RS12630	23.3	*NA*
sid2	non-ribosomal peptide	*NA*	RS13260-RS13385	40.7	*NA*
sid3	non-ribosomal peptide	*NA*	RS13985-RS14120	29.2	*NA*
sid4	non-ribosomal peptide	*NA*	RS14125-RS14260	40.8	*NA*
bac2	ribosomal peptide	*NA*	RS14265-RS15290	19.0	*NA*
pks4	polyketide	*NA*	RS21120-RS21540	10.0	*NA*
nrps2	non-ribosomal peptide	*NA*	RS22250-RS22350	34.7	*NA*

696

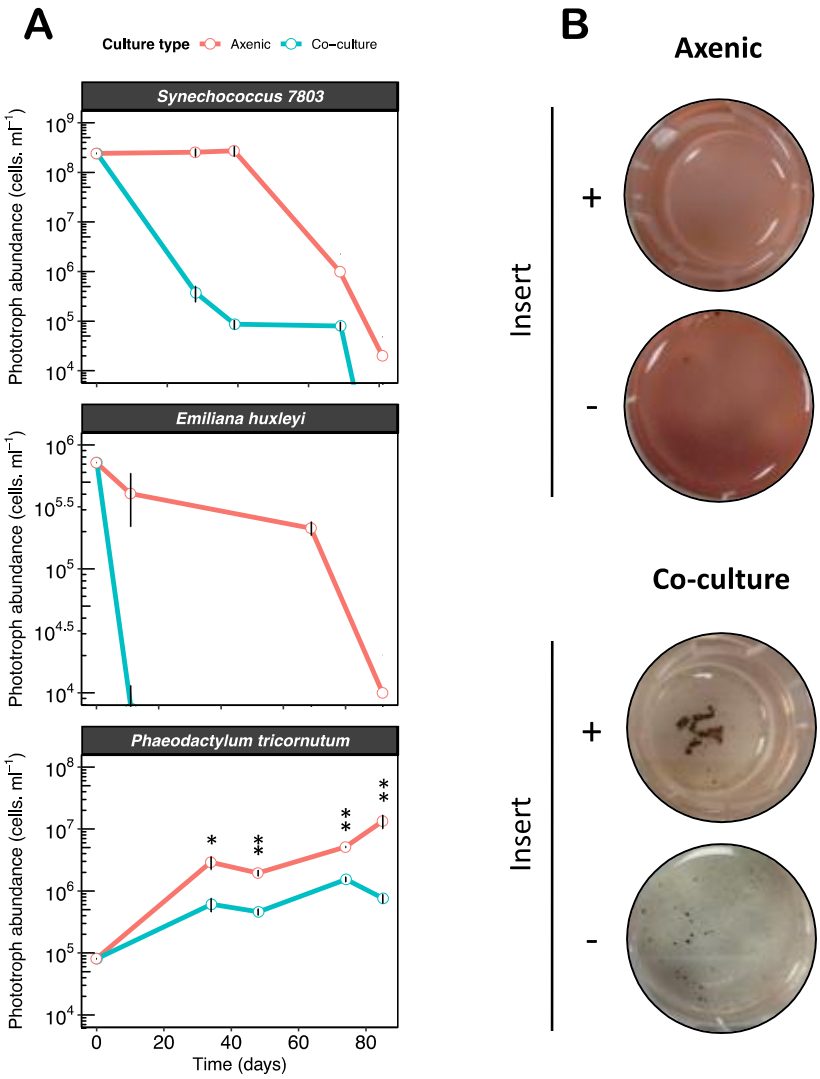

Figure 1 | *Salinispora tropica* inhibits the growth of marine phototrophs *via* the secretion of an antimicrobial molecule (A) *S. tropica* inhibits marine phototrophs growth in co-culture. Cultures of three marine phototrophs grown axenically (red lines) and in co-culture with *Salinispora tropica* (blue lines). Graph shows mean ± standard deviation of three biological replicates. Statistically significant cell abundances are indicated (T-test, significant * at *p*-value < 0.05 and ** at *p*-value < 0.01). **(B)** *Synechococcus* growth inhibition by *S. tropica* mediated by a diffusible molecule. The cyanobacterium was grown axenically and in co-culture with *S. tropica,* separated by a 0.4 µm pore membrane insert. Photographs of representative cultures of three biological replicates are shown, 7 days after inoculation. Red pigmentation is characteristic of healthy *Synechococcus* cells, while cell bleaching indicates cell death.

697

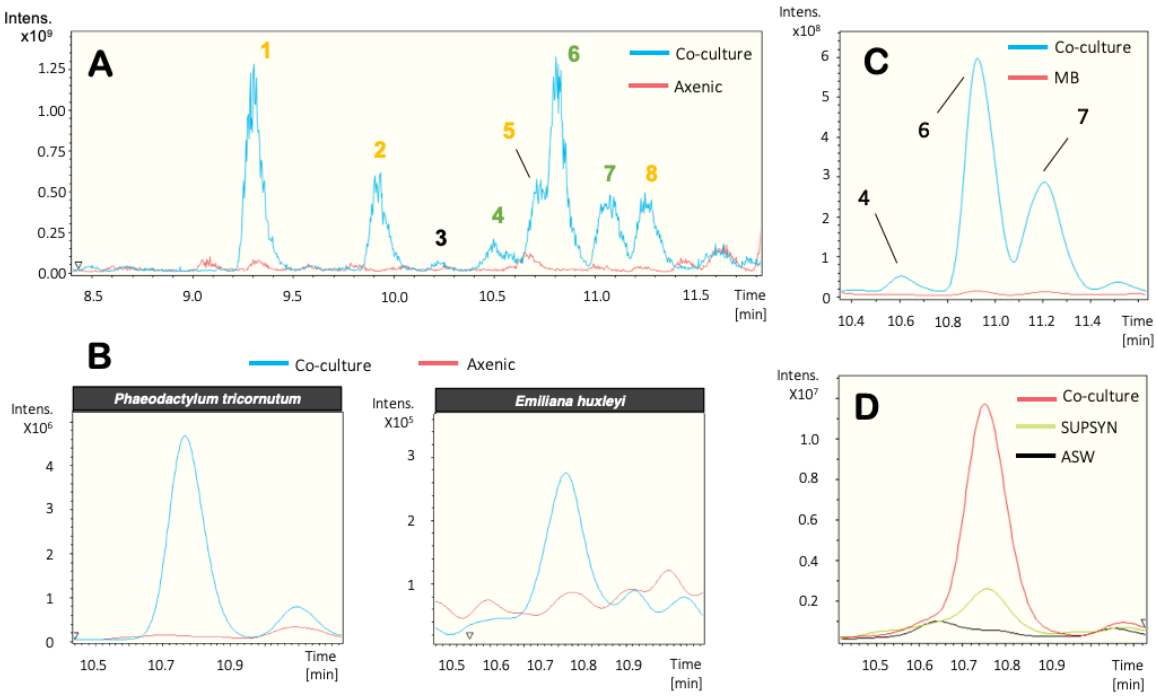

Figure 2 | Marine phototrophs trigger the production of cryptic molecules in *S. tropica* **(A)** *S. tropica* produces detectable small molecules in co-culture with *Synechococcus*. Overlaid base peak chromatograms (BPCs) of *Synechococcus* culture concentrated supernatants, when grown in artificial sea water (ASW) either axenically (red) or in co-culture with *S. tropica* (blue). Peaks characteristic of the co-culture condition are labelled from **1** to **8**. Color of the labels indicate groups of related compounds. **(B)** Other marine phototrophs also trigger the production of metabolite **6** by *S. tropica* as observed in panel A. Figure shows extracted ion chromatograms for the molecule **6** EIC 435.2 ± 0.1 in the supernatants of the phototrophs grown axenically (red) and in co-culture with *S. tropica* (blue). **(C)** The production of the related molecules **4**, **6** and **7** is dependent on the presence of photosynthate rather than high-nutrient availability. Graph shows extracted ion chromatograms for all three cryptic molecules EIC (464.2; 435.2; 449.2) ± 0.5 in the concentrated supernatants of *S. tropica* grown axenically in marine broth (MB, red) or in co-culture with *Synechococcus* in ASW (Co-culture, blue). **(D)** Cryptic molecule production is triggered by nutrients released by *Synechococcus* rather than cell-to-cell interactions. Graph shows extracted ion chromatograms for the cryptic molecule **6** (EIC 435.2 ± 0.5) in the supernatant of *S. tropica* grown axenically either in artificial sea water (ASW, black line) or in a conditioned *Synechococcus* supernatant (SUPSYN, green line); and in co-culture with *Synechococcus* (Co-culture, red line).

Table 2 | Characteristics of the cryptic molecules. MS Peak numbering is based on HPLC retention time. High-resolution LC-(+)ESI-MS *m/z* values and predicted chemical formulae for $[M+H]^+$ are provided.

MS Peak	Observed *m/z*	Chemical formulae for $[M+H]^+$ (calculated *m/z*; err [ppm])	MS/MS
3	438.1701	$[C_{28}H_{24}NO_4]^+$ (438.1700; -0.3)	194.0817
			177.1279
4	464.2509	$[C_{22}H_{34}N_5O_6]^+$ (464.2504; -1.2)	**276.1600**
			171.0880
			154.0615
6	435.2609	$[C_{22}H_{35}N_4O_5]^+$ (435.2602; -1.7)	372.2290
			276.1599
			142.0979
7	449.2764	$[C_{23}H_{37}N_4O_5]^+$ (449.2758; -1.3)	156.1135

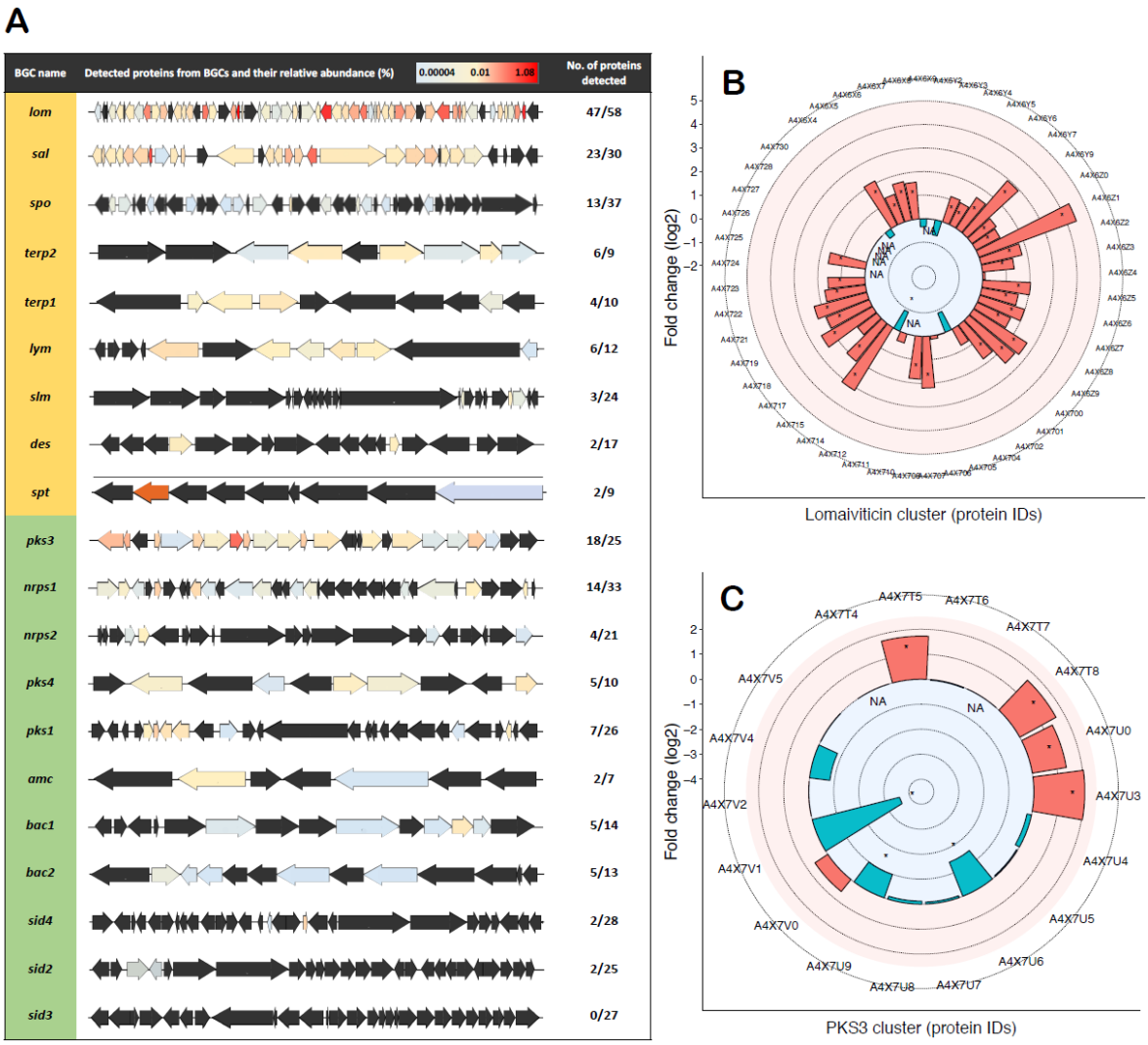

Figure 3 | Photosynthate activates orphan biosynthetic gene clusters in *S. tropica*. (A) Characterized (orange) and orphan BGCs (green) in *S. tropica* CNB-440 detected by high-throughput proteomics when grown with photosynthate (SUPSYN). Genes are colored according to the relative abundance of their corresponding proteins. Those that were not detected are represented in black. Photosynthate increased the detection of proteins involved in the production of lomaiviticin **(B)** and the orphan PKS3 **(C)** in comparison with cells grown in MB. Up- (red) and down-regulated (blue) proteins in the presence of the photosynthate is shown. Statistically significant fold changes are indicated by an asterisk (T-test, significant at *q*-value < 0.05). *NA* indicate proteins for which the T-test and fold change could not be estimated because of missing values within a set of replicates.

Table 3 | Detected proteins from the *nrps1* orphan BGC in *S. tropica* CNB-440 grown with photosynthate. Proteins involved in non-ribosomal peptide biosynthesis and antibiotic self-resistance are highlighted in bold.

Protein ID	Annotation	Relative abundance (%; n = 3)
A4X2P5	RidA family protein	0.014
A4X2P8	MFS transporter	0.011
A4X2Q0	**non-ribosomal peptide synthetase**	**0.004**
A4X2Q2	SDR family oxidoreductase	0.002
A4X2R0	acyl-CoA dehydrogenase	0.005
A4X2R1	acyl-CoA dehydrogenase	0.001
A4X2R4	D-alanine--poly(phosphoribitol) ligase	0.004
A4X2R5	**condensation domain-containing protein**	**0.001**
A4X2R7	argininosuccinate synthase	0.001
A4X2R8	methionyl-tRNA formyltransferase	0.087
A4X2S2	**ATP-dependent Clp protease proteolytic subunit**	**0.121**
A4X2S4	potassium channel family protein	0.002
A4X2S5	2-oxoacid:ferredoxin oxidoreductase subunit beta	0.006
A4X2S6	2-oxoacid:acceptor oxidoreductase subunit alpha	0.004

718
719
720
721
722
723
724
725
726

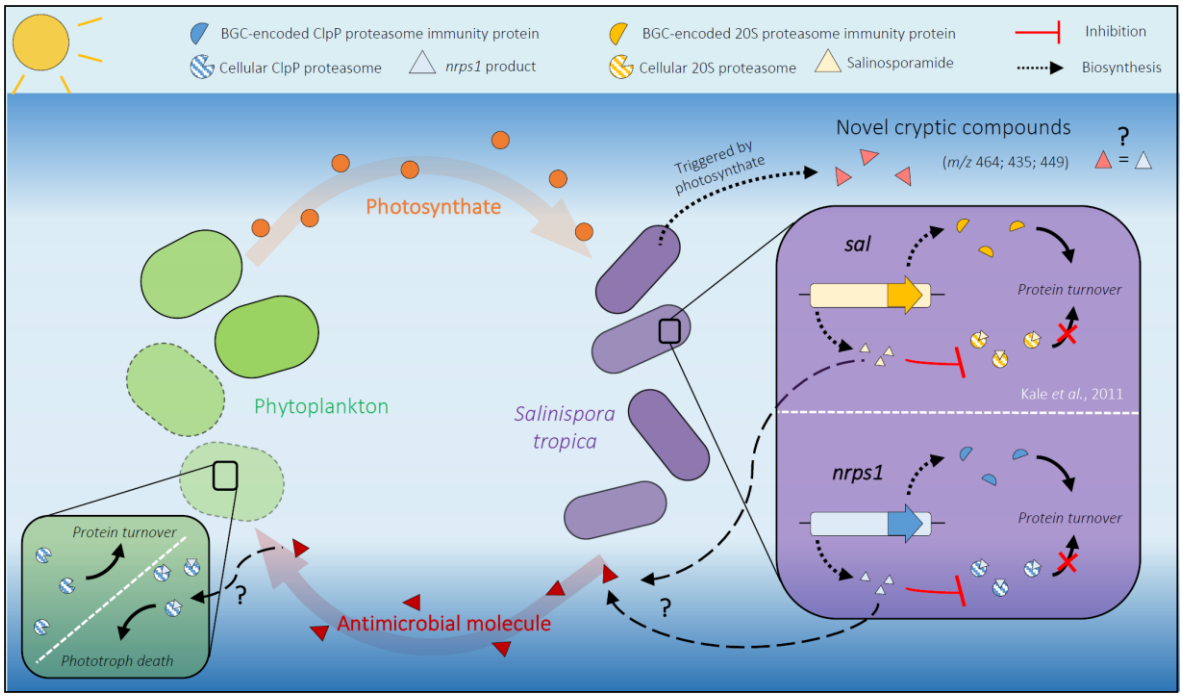

Figure 4 | Interaction of *Salinispora tropica* with phytoplankton. Marine phototrophs release photosynthate that triggers the biosynthesis of novel cryptic metabolites in *S. tropica*. *S. tropica* produces an unknown antimicrobial molecule that kills phytoplankton. The proposed mechanism of the antimicrobial metabolite as well as the activity of the *nrps1* product are depicted (green and purple boxes, respectively). The BGC *nrps1* would produce a ClpP-proteasome inhibitor, to which *S. tropica* would be resistant because of an immunity protein encoded within the BGC, similarly to what is known for *sal*/salinosporamide. The *nrps1*-encoded proteasome inhibitor could kill the phototrophs by preventing protein turnover, leading to cell death.

727